

## DIFFERENTIAL FORMS INSPIRED DISCRETIZATION FOR FINITE ELEMENT ANALYSIS OF INHOMOGENEOUS WAVEGUIDES

Qi I. Dai<sup>1, 2</sup>, Weng Cho Chew<sup>2, \*</sup>, and Li Jun Jiang<sup>1</sup>

<sup>1</sup>The University of Hong Kong, Pok Fu Lam Road, Hong Kong, China

<sup>2</sup>University of Illinois at Urbana-Champaign, Urbana, IL 61801, USA

**Abstract**—We present a differential forms inspired discretization for variational finite element analysis of inhomogeneous waveguides. The variational expression of the governing equation involves transverse fields only. The conventional discretization with edge elements yields an unsolvable generalized eigenvalue problem since one of the sparse matrix is singular. Inspired by the differential forms where the Hodge operator transforms 1-forms to 2-forms, we propose to discretize the electric and magnetic field with curl-conforming basis functions on the primal and dual grid, and discretize the magnetic flux density and electric displacement field with the divergence-conforming basis functions on the primal and dual grid, respectively. The resultant eigenvalue problem is well-conditioned and easy to solve. The proposed scheme is validated by several numerical examples.

### 1. INTRODUCTION

Since their introduction in the early 20th century, electromagnetic waveguides have been intensively studied, and find a variety of applications at different frequency bands ranging from radio-frequency (RF) and microwaves up to optical frequencies [1]. Advances in waveguides technology have called for numerical analysis of various wave guiding structures, e.g., metallic waveguides, microstrip lines and fiber optics. To list a few, [2] used a combination of numerical and analytical methods to solve for the waveguide eigenmodes; [3] and [4] used surface and volume integral equation methods to solve dielectric waveguide problems, respectively; finite-difference [5–10] and

---

*Received 18 October 2013, Accepted 9 January 2014, Scheduled 17 January 2014*

\* Corresponding author: Weng Cho Chew (w-chew@uiuc.edu).

Invited paper dedicated to the memory of Robert E. Collin.

finite element [11–18] techniques are powerful and flexible in modeling a wide variety of waveguides.

In the finite element related publications, Cendes and Silvester [11], and Ahmed and Daly [12] solved the problem with  $E_z$ - $H_z$  formulation which suffers from the occurrence of spurious modes. This difficulty was overcome by using the transverse field formulation [7, 13]. For example, Nasir and Chew [13] presented a variational analysis of anisotropic and inhomogeneous waveguides where only transverse fields are involved. Their method is limited by the usage of nodal basis functions which fail to deal with structures with sharp discontinuities. Lee [18] proposed a hybrid finite element analysis where the transverse and  $z$  components of the electric field are discretized with edge elements and nodal basis functions, respectively. This hybrid formulation results in a larger eigenvalue problem to solve since the unknowns for  $E_z$  are also included.

The variational expression suggested in [13, 20, 21] has the beauty of mathematical symmetry and clear physical meaning in each of its terms. However, the edge element based discretization for this variational problem is rarely documented in the literature. One possible reason is that the divergence terms in the variational form require the basis functions to be divergence-conforming while edge elements used to expand the fields are curl-conforming. Also, a naive implementation of the vector basis functions results in a singular matrix giving rise to an unsolvable generalized eigenvalue problem. Fortunately, these difficulties can be overcome by using a differential forms inspired discretization. Differential forms has been increasingly adopted in deriving stable FEM schemes in recent years. Hopefully, it will serve as useful guidance on the finite element discretization in complicated variational problems. In this paper, we adopt notations of differential forms in Section 2.2. The rest sections are written in notations of vector calculus.

## 2. FORMULATIONS

### 2.1. Variational Eigenvalue Problem

It follows from [13, 20, 21] that the governing wave equation for an inhomogeneous and anisotropic waveguide is

$$\nabla \times \bar{\boldsymbol{\mu}}^{-1} \cdot \nabla \times \mathbf{E} - \omega^2 \bar{\boldsymbol{\epsilon}} \cdot \mathbf{E} = 0, \quad (1)$$

where the waveguide is assumed to have reflection symmetry in the propagation  $z$  direction such that [19, 21]

$$\bar{\boldsymbol{\epsilon}} = \begin{bmatrix} \bar{\epsilon}_s & 0 \\ 0 & \epsilon_{zz} \end{bmatrix}, \quad (2)$$

and

$$\bar{\boldsymbol{\mu}} = \begin{bmatrix} \bar{\boldsymbol{\mu}}_s & 0 \\ 0 & \mu_{zz} \end{bmatrix}. \tag{3}$$

Using the divergence condition

$$ik_z E_z = -\epsilon_{zz}^{-1} \nabla_s \cdot \bar{\boldsymbol{\epsilon}}_s \cdot \bar{\mathbf{E}}_s \tag{4}$$

to eliminate  $E_z$ , the transverse electric field  $\mathbf{E}_s$  satisfies

$$\begin{aligned} \bar{\boldsymbol{\mu}}_s \cdot \hat{z} \times \nabla_s \times \mu_{zz}^{-1} \nabla_s \times \mathbf{E}_s - \hat{z} \times \nabla_s \epsilon_{zz}^{-1} \nabla_s \cdot \bar{\boldsymbol{\epsilon}}_s \cdot \mathbf{E}_s \\ - \omega^2 \bar{\boldsymbol{\mu}}_s \cdot \hat{z} \times \bar{\boldsymbol{\epsilon}}_s \cdot \mathbf{E}_s + k_z^2 \hat{z} \times \mathbf{E}_s = 0 \end{aligned} \tag{5}$$

The transpose equation of (5) is given by

$$\begin{aligned} \bar{\boldsymbol{\epsilon}}_s^t \cdot \hat{z} \times \nabla_s \times \epsilon_{zz}^{-1} \nabla_s \times \mathbf{H}_s^a - \hat{z} \times \nabla_s \mu_{zz}^{-1} \nabla_s \cdot \bar{\boldsymbol{\mu}}_s^t \cdot \mathbf{H}_s^a \\ - \omega^2 \bar{\boldsymbol{\epsilon}}_s^t \cdot \hat{z} \times \bar{\boldsymbol{\mu}}_s^t \cdot \mathbf{H}_s^a + k_z^2 \hat{z} \times \mathbf{H}_s^a = 0 \end{aligned} \tag{6}$$

The variational expression for eigenvalue problems (5) and (6) is

$$-k_z^2 = \frac{\langle \mathbf{H}_s^a, \mathcal{L} \mathbf{E}_s \rangle}{\langle \mathbf{H}_s^a, \mathcal{B} \mathbf{E}_s \rangle}, \tag{7}$$

where

$$\mathcal{L} = \bar{\boldsymbol{\mu}}_s \cdot \hat{z} \times \nabla_s \times \mu_{zz}^{-1} \nabla_s \times - \hat{z} \times \nabla_s \epsilon_{zz}^{-1} \nabla_s \cdot \bar{\boldsymbol{\epsilon}}_s \cdot - \omega^2 \bar{\boldsymbol{\mu}}_s \cdot \hat{z} \times \bar{\boldsymbol{\epsilon}}_s \cdot, \tag{8a}$$

$$\mathcal{B} = \hat{z} \times. \tag{8b}$$

The reaction inner product is define as  $\langle \mathbf{f}, \mathbf{g} \rangle = \int_S \mathbf{f} \cdot \mathbf{g} \, d\Omega$  where  $S$  is the cross section of the waveguide. Moreover, it is easy to find the transpose operators of  $\mathcal{L}$  and  $\mathcal{B}$  to be

$$\mathcal{L}^t = -\bar{\boldsymbol{\epsilon}}_s^t \cdot \hat{z} \times \nabla_s \times \epsilon_{zz}^{-1} \nabla_s \times + \hat{z} \times \nabla_s \mu_{zz}^{-1} \nabla_s \cdot \bar{\boldsymbol{\mu}}_s^t \cdot + \omega^2 \bar{\boldsymbol{\epsilon}}_s^t \cdot \hat{z} \times \bar{\boldsymbol{\mu}}_s^t \cdot, \tag{9a}$$

$$\mathcal{B}^t = -\hat{z} \times. \tag{9b}$$

Hence, We can write Equation (7) as

$$\begin{aligned} -\langle \mathbf{H}_s^a, \hat{z} \times \mathbf{E}_s \rangle k_z^2 &= -\langle \hat{z} \nabla_s \cdot \bar{\boldsymbol{\mu}}_s^t \cdot \mathbf{H}_s^a, \mu_{zz}^{-1} \nabla_s \times \mathbf{E}_s \rangle \\ &+ \langle \epsilon_{zz}^{-1} \nabla_s \times \mathbf{H}_s^a, \hat{z} \nabla_s \cdot \bar{\boldsymbol{\epsilon}}_s \cdot \mathbf{E}_s \rangle \\ &- \omega^2 \langle \mathbf{H}_s^a, \bar{\boldsymbol{\mu}}_s \cdot \hat{z} \times \bar{\boldsymbol{\epsilon}}_s \cdot \mathbf{E}_s \rangle \end{aligned} \tag{10}$$

A straightforward implementation of the vector basis functions is to expand both transverse fields  $\mathbf{E}_s$  and  $\mathbf{H}_s^a$  in Equation (10) with the 2-D curl-conforming Rao-Wilton-Glisson (RWG) elements [32] (edge elements)  $\mathbf{w}_j$ . Since the divergence terms in Equation (10) prohibit the direct use of curl-conforming RWG's, the transverse  $\bar{\boldsymbol{\epsilon}}_s \cdot \mathbf{E}_s$  and  $\bar{\boldsymbol{\mu}}_s^t \cdot \mathbf{H}_s^a$  are expanded with divergence-conforming RWG's  $\mathbf{f}_j = \hat{z} \times \mathbf{w}_j$ . The main problem of this discretization scheme is that the matrix resulted from  $\langle \mathbf{H}_s^a, \hat{z} \times \mathbf{E}_s \rangle$  is singular, where the diagonal entries  $\langle \mathbf{f}_j, \hat{z} \times \mathbf{f}_j \rangle$  are all zero.

## 2.2. Differential Forms

In differential forms [22–30], Maxwell’s equations (source-free case) are written as

$$dE = i\omega B, \quad (11a)$$

$$dB = 0, \quad (11b)$$

$$dH = -i\omega D, \quad (11c)$$

$$dD = 0, \quad (11d)$$

where  $E$  and  $H$  are electric and magnetic intensity 1-forms;  $D$  and  $B$  are electric and magnetic flux 2-forms;  $d$  is the metric-free exterior derivative operator [25, 30]. The constitutive relations are written in terms of Hodge operators as  $D = \star_{\epsilon} E$  and  $H = \star_{\mu^{-1}} B$ , where the continuum Hodge (star) operators give rise to an isomorphism between  $p$ -forms and  $(n - p)$ -forms in a  $n$ -dimensional space [24].

On the discrete level, both the 1-form  $E$  and 2-form  $D$  cannot be represented simultaneously in the same mesh [24]. The remedy is to assign  $E$  and  $D$  on a pair of dual grids, which also applies to  $H$  and  $B$ . In 3-D applications [24, 30],  $E$  is associated with primal edges (1-cells), and  $B$  is associated with primal faces (2-cells), where the primal grid is a cell complex which can be simplices, rectangular boxes, polyhedra, and so on. In the dual lattice which yields one-to-one correspondence with the primal one between  $p$ -cells and  $(n - p)$ -cells,  $H$  is associated with dual edges (1-cells), and  $D$  is associated with dual faces (2-cells). The dual grid of a simplicial mesh can be chosen based on a barycentric subdivision, or in some cases, based on a Delaunay-Voronoi construction [24].

One can discretize Maxwell’s equations (11) by expanding  $E$  and  $B$  with Whitney forms as [31]

$$E = \sum_j e_j W_j^1, \quad (12a)$$

$$B = \sum_j b_j W_j^2, \quad (12b)$$

where  $W_j^p$  is the Whitney  $p$ -form associated with the  $i$ th  $p$ -cell. The discrete constitutive equations are written as

$$\mathbb{D} = [\star_{\epsilon}] \mathbb{E}, \quad (13a)$$

$$\mathbb{H} = [\star_{\mu^{-1}}] \mathbb{B}, \quad (13b)$$

where  $\mathbb{E}$ ,  $\mathbb{H}$ ,  $\mathbb{D}$ , and  $\mathbb{B}$  are column vectors whose elements are the degrees of freedom (DoFs) of the problem, and the discrete Hodge

operators have entries as

$$[\star\epsilon]_{ij} = \int_{\Omega} \epsilon W_i^1 \wedge \star W_j^1, \tag{14a}$$

$$[\star\mu^{-1}]_{ij} = \int_{\Omega} \frac{1}{\mu} W_i^2 \wedge \star W_j^2, \tag{14b}$$

where  $\wedge$  is the exterior product.

### 2.3. Differential Forms Inspired Discretization

To implement the variational finite element analysis of inhomogeneous and anisotropic waveguides, we apply the Rayleigh-Ritz procedure to Equation (10). Inspired by the differential forms, in terms of vector calculus, we expand the transverse fields  $\mathbf{E}_s$  with curl-conforming primal basis functions  $\mathbf{w}_j$  as

$$\mathbf{E}_s = \sum_{j=1}^N e_j \mathbf{w}_j, \tag{15}$$

and  $\mathbf{H}_s^a$  with curl-conforming dual basis functions  $\tilde{\mathbf{w}}_j$  as

$$\mathbf{H}_s^a = \sum_{j=1}^N h_j \tilde{\mathbf{w}}_j. \tag{16}$$

On the other hand, we expand transverse  $\bar{\boldsymbol{\mu}}_s^t \cdot \mathbf{H}_s^a$  with divergence-conforming primal basis functions  $\mathbf{f}_j$  as

$$\bar{\boldsymbol{\mu}}_s^t \cdot \mathbf{H}_s^a = \sum_{j=1}^N b_j \mathbf{f}_j, \tag{17}$$

and  $\bar{\boldsymbol{\epsilon}}_s \cdot \mathbf{E}_s$  with divergence-conforming dual basis functions  $\tilde{\mathbf{f}}_j$  as

$$\bar{\boldsymbol{\epsilon}}_s \cdot \mathbf{E}_s = \sum_{j=1}^N d_j \tilde{\mathbf{f}}_j. \tag{18}$$

We choose  $\mathbf{f}_j$  and  $\tilde{\mathbf{f}}_j$  to be RWG basis functions [32] and Buffa-Christiansen (BC) basis functions [33], respectively, both of which are divergence-conforming, and can be considered as the 2-D vector calculus version of Whitney 2-forms  $W_j^2$  on the primal and dual grids, respectively<sup>†</sup>. The divergence-conforming and curl-conforming basis

---

<sup>†</sup> Another possibility is to use Chen-Wilton (CW) basis functions [34].

functions satisfy

$$\mathbf{f}_j = \hat{z} \times \mathbf{w}_j, \tag{19a}$$

$$\tilde{\mathbf{f}}_j = \hat{z} \times \tilde{\mathbf{w}}_j, \tag{19b}$$

where  $\mathbf{w}_j$  and  $\tilde{\mathbf{w}}_j$  can be considered as the 2-D vector calculus version of Whitney 1-forms  $W_j^1$  on the primal and dual grids, respectively.

Defined on the primal grid, the curl-conforming RWG's  $\mathbf{w}_j$  and the divergence-conforming RWG's  $\mathbf{f}_j$  are illustrated in Figures 1(a) and (b), respectively. On the other hand, the dual basis function is constructed on the barycentric mesh. Defined on the dual grid, the curl-conforming BC's  $\tilde{\mathbf{w}}_j$  and the divergence-conforming BC's  $\tilde{\mathbf{f}}_j$  are illustrated in Figures 2(a) and (b), respectively. Also of note is that  $\tilde{\mathbf{w}}_j$  is quasi-divergence-conforming, while  $\tilde{\mathbf{f}}_j$  is quasi-curl-conforming.

Testing both sides of (18) with  $\mathbf{w}_i$  yields

$$\sum_j \langle \mathbf{w}_i, \bar{\epsilon}_s \cdot \mathbf{w}_j \rangle e_j = \sum_j \langle \mathbf{w}_i, \tilde{\mathbf{f}}_j \rangle d_j, \quad i = 1, \dots, N, \tag{20}$$

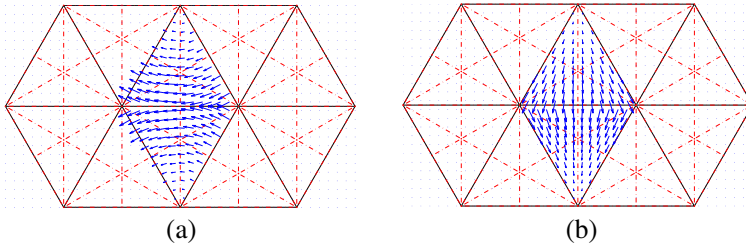


**Figure 1.** Basis functions on the primal grid. (a) Curl-conforming RWG's (edge elements)  $\mathbf{w}_i$ . (b) Divergence-conforming RWG's  $\mathbf{f}_i$ .

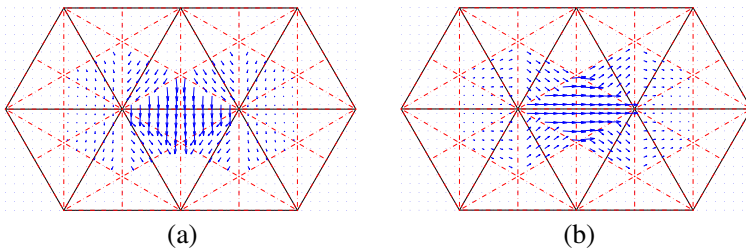


**Figure 2.** Basis functions on the dual grid. (a) Curl-conforming and quasi-divergence-conforming BC's  $\tilde{\mathbf{w}}_i$ . (b) Divergence-conforming and quasi-curl-conforming BC's  $\tilde{\mathbf{f}}_i$ .

or more compactly, in a matrix form as

$$[\star_\epsilon] \cdot \mathbb{E} = [\mathbf{G}] \cdot \mathbb{D}, \tag{21}$$

where the discrete Hodge operator  $[\star_\epsilon]$  has elements

$$[\star_\epsilon]_{ij} = \langle \mathbf{w}_i, \bar{\epsilon}_s \cdot \mathbf{w}_j \rangle, \tag{22}$$

which are consistent with their 3-D differential forms counterparts (14a). The Gramian matrix  $[\mathbf{G}]$  has elements

$$[\mathbf{G}]_{ij} = \langle \mathbf{w}_i, \tilde{\mathbf{f}}_j \rangle, \tag{23}$$

which are consistent with those obtained in the multiplicative Calderon preconditioner for integral equation problems [35]. Moreover, the arrays of DoFs on primal and dual grids  $\mathbb{E}$  and  $\mathbb{D}$  have elements  $e_j$  and  $d_j$ , respectively. Thus, we have

$$\mathbb{D} = [\mathbf{G}]^{-1} \cdot [\star_\epsilon] \cdot \mathbb{E}. \tag{24}$$

Similarly, we can obtain

$$[\star_\mu] \cdot \mathbb{H} = -[\mathbf{G}]^t \cdot \mathbb{B}, \tag{25}$$

or

$$\mathbb{B} = -([\mathbf{G}]^t)^{-1} \cdot [\star_\mu] \cdot \mathbb{H}, \tag{26}$$

where the discrete Hodge operator  $[\star_\mu]$  has elements

$$[\star_\mu]_{ij} = \langle \tilde{\mathbf{w}}_i, \bar{\mu}_s^t \cdot \tilde{\mathbf{w}}_j \rangle, \tag{27}$$

and the arrays of DoFs on primal and dual grids  $\mathbb{B}$  and  $\mathbb{H}$  have elements  $b_j$  and  $h_j$ , respectively. Here,  $[\mathbf{G}]^{-1}$  can be replaced with the sparse approximate inverse of  $[\mathbf{G}]$ , detail of which is provided in Appendix A.

Substituting Equations (15) to (17) into (10), we have

$$\begin{aligned} & - \langle \hat{z} \nabla_s \cdot \bar{\mu}_s^t \cdot \mathbf{H}_s^a, \mu_{zz}^{-1} \nabla_s \times \mathbf{E}_s \rangle \\ &= - \left\langle \hat{z} \nabla_s \cdot \sum_j b_j \mathbf{f}_j, \mu_{zz}^{-1} \nabla_s \times \sum_j e_j \mathbf{w}_j \right\rangle \\ &= -\mathbb{B}^t \cdot [\mathbf{K}_1] \cdot \mathbb{E} = \mathbb{H}^t \cdot [\star_\mu]^t \cdot [\mathbf{G}]^{-1} \cdot [\mathbf{K}_1] \cdot \mathbb{E} = \mathbb{H}^t \cdot [\mathbf{L}_1] \cdot \mathbb{E} \end{aligned} \tag{28}$$

where  $[\mathbf{L}_1] = [\star_\mu]^t \cdot [\mathbf{G}]^{-1} \cdot [\mathbf{K}_1]$ , and matrix  $[\mathbf{K}_1]$  has elements  $[\mathbf{K}_1]_{ij} = \langle \hat{z} \nabla_s \cdot \mathbf{f}_i, \mu_{zz}^{-1} \nabla_s \times \mathbf{w}_j \rangle$ .

Similarly, we have

$$\langle \epsilon_{zz}^{-1} \nabla_s \times \mathbf{H}_s^a, \hat{z} \nabla_s \cdot \bar{\epsilon}_s \cdot \mathbf{E}_s \rangle = \mathbb{H}^t \cdot [\mathbf{L}_2] \cdot \mathbb{E}, \tag{29}$$

$$-\omega^2 \langle \mathbf{H}_s^a, \bar{\mu}_s \cdot \hat{z} \times \bar{\epsilon}_s \cdot \mathbf{E}_s \rangle = \mathbb{H}^t \cdot [\mathbf{L}_3] \cdot \mathbb{E}, \tag{30}$$

$$\langle \mathbf{H}_s^a, \hat{z} \times \mathbf{E}_s \rangle = \mathbb{H}^t \cdot [\mathbf{B}] \cdot \mathbb{E}, \tag{31}$$

where  $[L_2] = [K_2] \cdot [G]^{-1} \cdot [\star_\epsilon]$ , and matrix  $[K_2]$  has elements that  $[K_2]_{ij} = \langle \epsilon_{zz}^{-1} \nabla_s \times \tilde{\mathbf{w}}_i, \hat{z} \nabla_s \cdot \tilde{\mathbf{f}}_j \rangle$ , and moreover,  $[L_3]_{ij} = -\omega^2 \langle \tilde{\mathbf{w}}_i, \bar{\boldsymbol{\mu}}_s \cdot \hat{z} \times \bar{\boldsymbol{\epsilon}}_s \cdot \mathbf{w}_j \rangle$ , and  $[B]_{ij} = \langle \tilde{\mathbf{w}}_i, \mathbf{f}_j \rangle$ .

Hence, the discrete variational problem of (7) can be written as

$$-k_z^2 = \frac{\mathbb{H}^t \cdot [L] \cdot \mathbb{E}}{\mathbb{H}^t \cdot [B] \cdot \mathbb{E}}, \tag{32}$$

where  $[L] = [L_1] + [L_2] + [L_3]$ . We require that the first variations of Equation (32) with respect to the  $e_j$ 's and  $h_j$ 's vanish. The optimal solution of the variational problem is then given by the solution of the following eigenvalue problems

$$([L] + k_z^2[B]) \cdot \mathbb{E} = 0, \tag{33}$$

$$([L]^t + k_z^2[B]^t) \cdot \mathbb{H} = 0, \tag{34}$$

where  $[L]^t$  and  $[B]^t$  can also be obtained by using Equations (9a), (9b), (15) to (18).

### 3. NUMERICAL RESULTS

#### 3.1. Circularly Cylindrical Waveguide

The radius of the circularly cylindrical waveguide is set to  $a = 1$  mm. Totally 1,938 triangular elements are generated by ANSYS, and the

**Table 1.** First few lowest eigenvalues  $k_s$  of circularly cylindrical waveguide.

Mode	Computed ( $\times 10^3$ )	Analytical ( $\times 10^3$ )	Error (%)
TE <sub>11</sub> <sup>(1)</sup>	1.8631	1.8412	1.19
TE <sub>11</sub> <sup>(2)</sup>	1.8624	1.8412	1.15
TM <sub>01</sub>	2.4417	2.4048	1.53
TE <sub>21</sub> <sup>(1)</sup>	3.0952	3.0542	1.34
TE <sub>21</sub> <sup>(2)</sup>	3.0951	3.0542	1.34
TE <sub>01</sub>	3.8576	3.8317	0.68
TM <sub>11</sub> <sup>(1)</sup>	3.8881	3.8317	1.47
TM <sub>11</sub> <sup>(2)</sup>	3.8876	3.8317	1.46
TE <sub>31</sub> <sup>(1)</sup>	4.2686	4.2012	1.60
TE <sub>31</sub> <sup>(2)</sup>	4.2688	4.2012	1.61
TM <sub>21</sub> <sup>(1)</sup>	5.2259	5.1356	1.76
TM <sub>21</sub> <sup>(2)</sup>	5.2251	5.1356	1.74

number of unknowns is 2,853. By setting the working frequency to zero, eigenvalues  $k_s$  are the  $n$ th root of  $J_m(x) = 0$  or  $J'_m(x) = 0$  where  $J_m(x)$  are Bessel functions of the first kind. The superscripts <sup>(1)</sup> and <sup>(2)</sup> denote the degeneracy. The first few computed eigenvalues  $k_s$  and the analytical values are given in Table 1. The electric field distributions of several modes are illustrated in Figure 3. We then obtain the  $k_z a$ - $k_0 a$  diagram for several guided modes in Figure 4, where the computed results (red squares) agree well with the theoretical results (solid lines).

### 3.2. Rectangular Dielectric Waveguide

We model a rectangular dielectric waveguide enclosed by a large PEC box with the proposed variational analysis. The aspect ratio is set to

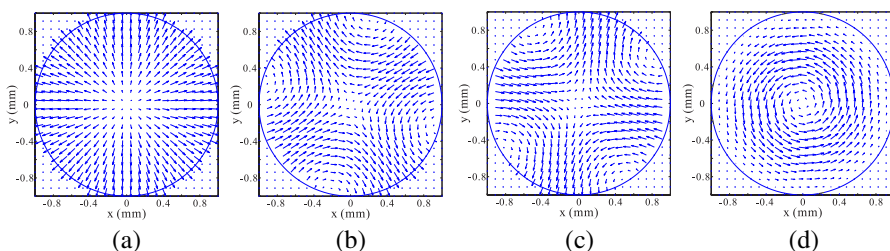


**Figure 3.** Examples of eigenmodes in a circularly cylindrical waveguide. (a)  $TM_{01}$ . (b)  $TE_{21}^{(1)}$ . (c)  $TE_{21}^{(2)}$ . (d)  $TE_{01}$ .

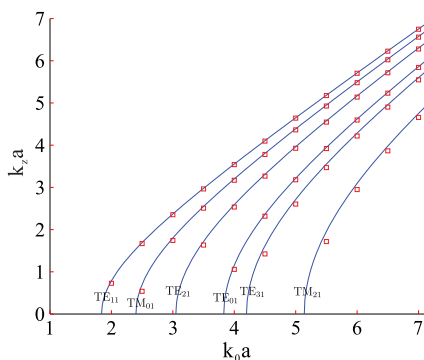


**Figure 4.**  $k_z a$ - $k_0 a$  diagram for guided modes in a circularly cylindrical waveguide.

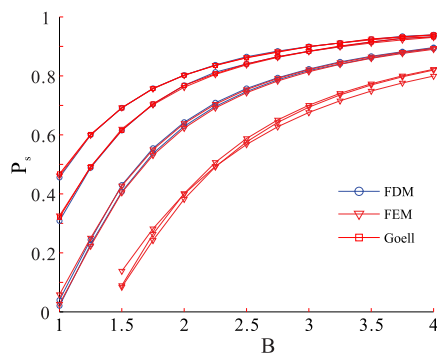


**Figure 5.** Dispersion curves for the lowest few propagating modes in a rectangular dielectric waveguide.

2, and the permittivity is  $\epsilon_r = 2.25$ . The results obtained by our FEM method agree well with those calculated by FDM [9] and Goell [37], as shown in Figure 5. Here, parameters  $P_s$  and  $B$  are defined as

$$P_s = \frac{k_z^2 - k_0^2}{k_1^2 - k_0^2}, \tag{35a}$$

$$B = \frac{b}{\pi} \sqrt{k_1^2 - k_0^2}, \tag{35b}$$

respectively.

### 3.3. Triple-conductor Stripline

The geometry of a multilayered triple-conductor stripline is shown in Figure 6, where we set  $\epsilon_1 = \epsilon_3 = 9.7\epsilon_0$ ,  $\epsilon_2 = 4\epsilon_0$ ,  $w/h = 1.0$ ,  $s/h = 0.1$ , and  $d = h$ . The dispersion curves obtained by the proposed FEM are in good agreement with those calculated by FDM [9] and by Yang et al. [38], as shown in Figure 7. The effective permittivity is computed as simple as

$$\epsilon_{eff} = \frac{k_z^2}{k_0^2}. \tag{36}$$

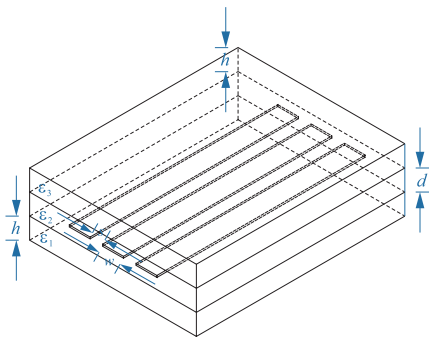


**Figure 6.** Triple-conductor stripline.

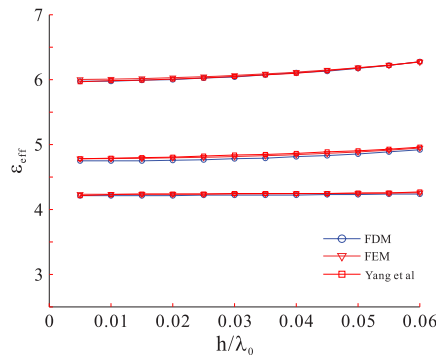


**Figure 7.** Dispersion curves for the triple-conductor stripline.

### 3.4. Dual-plate Triple Microstrip Structure

We analyze a dual-plate triple microstrip line as shown in Figure 8, with  $\epsilon_{x1} = \epsilon_{x2} = 9.4\epsilon_0$ ,  $\epsilon_{y1} = \epsilon_{y2} = 11.6\epsilon_0$ ,  $\epsilon_{z1} = \epsilon_{z2} = 9.4\epsilon_0$ ,  $h = 4.0$  mm,  $a = 10.0$  mm, and  $s = 2.0$  mm. The dispersion curves

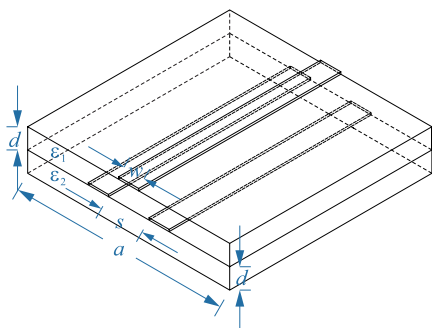


**Figure 8.** Dual plate triple microstrip structure.

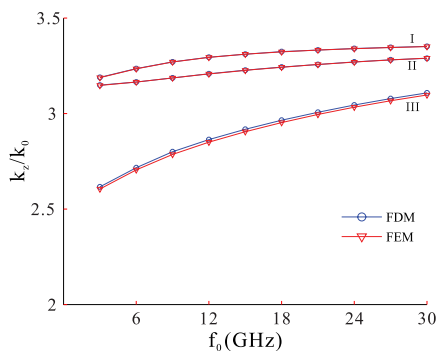


**Figure 9.** Dispersion curves for the dual plate triple microstrip structure.

**Table 2.** Normalized propagation constants computed by FDM and FEM.

Frequency (GHz)	FDM	FEM	Difference (%)
6	3.2321	3.2294	0.0835
12	3.2972	3.2949	0.0698
18	3.3337	3.3315	0.0660
24	3.3591	3.3571	0.0595
30	3.3795	3.3777	0.0533

computed by the proposed method and by the FDM [9] are in good agreement, as shown in Figure 9.

When some off-diagonal components in  $\bar{\epsilon}_s$  are introduced ( $\epsilon_{xy1} = \epsilon_{yx1} = 2.0\epsilon_0$ ), the normalized propagation constants  $k_z/k_0$  for mode I are computed by both the proposed FEM and Radhakrishnan’s FDM, where good agreements are shown in Table 2.

With a typical finite element discretization, the numbers of unknowns in the waveguide problems (from Section 3.3 to 3.6) are in the order of  $10^3$  to  $10^4$ , which are similar to those generated in Radhakrishnan’s publication [9]. The resulted generalized eigenvalue problems can be easily solved with the conventional eigensolvers such as Lanczos and Arnoldi methods. The MATLAB embedded ARPACK is applied to these problems, and the CPU times are only a few minutes even for a small computer.

#### 4. CONCLUSIONS

In this paper, a differential forms inspired discretization for variational finite element analysis of inhomogeneously loaded waveguides is proposed. In the variational expression which involves transverse fields only, the electric field  $\mathbf{E}_s$  and magnetic field  $\mathbf{H}_s$  are expanded with curl-conforming RWG's and curl-conforming BC's, respectively, while the electric displacement field  $\mathbf{D}_s$  and magnetic flux density  $\mathbf{B}_s^a$  are expanded with divergence-conforming BC's and divergence-conforming RWG's, respectively. The DoFs of  $\mathbf{D}_s$  and  $\mathbf{B}_s^a$  are connected to those of  $\mathbf{E}_s$  and  $\mathbf{H}_s$  by the Galerkin's discrete Hodges and the Gramian matrix. By using the sparse approximate inverse of the Gramian matrix, the resultant eigensystem involve sparse matrices only, which can be easily solved with conventional eigensolvers. Besides, this work offers useful insight that differential forms may serve as precise design rules for discretization in complicated variational problems.

#### APPENDIX A. SPARSE APPROXIMATE INVERSE

Matrix  $[A]$  has a good sparse approximate inverse  $[M]$  provided that most entries in  $[A]^{-1}$  are relatively small. An approach to finding  $[M]$  is to minimize

$$\|[A][M] - [I]\|_F^2 = \sum_{k=1}^N \|([A][M] - [I])\{e_\alpha\}\|_2^2, \quad (A1)$$

where the subscript  $F$  denotes the Frobenius norm, and  $\{e_\alpha\}$  is a column vector satisfying  $\{e_\alpha\}^t = (0, \dots, 0, 1, 0, \dots, 0)$  where the  $\alpha$ -th entry is 1. We cast such a problem into  $N$  independent least squares problems as

$$\min_{\{M_\alpha\}} \|[A]\{M_\alpha\} - \{e_\alpha\}\|_2, \quad \alpha = 1, \dots, N, \quad (A2)$$

where  $\{M_\alpha\}$  is the  $\alpha$ -th column of  $[M]$ . The above holds since the columns of  $[M]$  are independent of one another.

The procedure to compute  $\{M_\alpha\}$  is as follows [36]: First, one needs to prescribe a sparsity pattern for  $\{M_\alpha\}$ . In this work, we assume that the sparse approximate inverse of  $[G]$  has the same sparsity pattern of  $[G]$  or  $[G]^2$ . Next, we let  $\mathcal{J}$  be the set of indices  $j$  such that the  $j$ -th entry of column vector  $\{M_\alpha\}_j \neq 0$ . We denote the reduced vector  $\{M_\alpha\}_{\mathcal{J}}$  by  $\{\bar{M}_\alpha\}$ . We let  $\mathcal{I}$  be the set of indices  $i$  such that  $[A]_{i\mathcal{J}}$  is not identically zero. We denote the submatrix  $[A]_{\mathcal{I}\mathcal{J}}$  as  $[\bar{A}]$ , and  $\{e_\alpha\}_{\mathcal{I}}$  as  $\{\bar{e}_\alpha\}$ , respectively. Hence, solving (A2) is equivalent to solving

$$\min_{\{\bar{M}_\alpha\}} \|[\bar{A}]\{\bar{M}_\alpha\} - \{\bar{e}_\alpha\}\|_2. \quad (A3)$$

If the  $n_1 \times n_2$  matrix  $[\bar{A}]$  is full rank ( $[A]$  is nonsingular), we have

$$[\bar{A}] = [Q] \begin{bmatrix} [R] \\ [0] \end{bmatrix}, \quad (\text{A4})$$

which is the QR decomposition for  $[\bar{A}]$ . Let  $\{c\} = [Q]^t \{\bar{e}_\alpha\}$ , we can obtain

$$\{\bar{M}_\alpha\} = [R]^{-1} \{c\}_{1:n_2}. \quad (\text{A5})$$

The sparse approximate inverse  $[M]$  can be improved by augmenting its sparsity structure. More detail can be found in [36].

## ACKNOWLEDGMENT

The paper is dedicated to the memory of Prof. Robert E. Collin. The second author (WCC) has benefited from the works of Bob Collin harking back to his student days at MIT. WCC enjoys the books which Bob has written with physical lucidness. WCC has developed a lifelong interest in waveguide theory primarily due to Bob Collin's work in the area, and Bob Collin's tome on the subject. WCC was impressed by Bob Collin's clarity of mind when he had interacted with him in the past. Bob took time to correspond with WCC even though he was a rather junior professor then at U of Illinois. Hence, WCC is forever grateful to the energy that Bob has had and his care for junior professors in the field.

This work was supported in part by the National Science Foundation under Award Number 1218552, in part by the Research Grants Council of Hong Kong (GRF 711609 and 711508), and in part by the University Grants Council of Hong Kong (Contract No. AoE/P-04/08).

## REFERENCES

1. Collin, R. E., *Field Theory of Guided Waves*, IEEE Press, 1991.
2. Chew, W. C., "Analysis of optical and millimeter wave dielectric waveguide," *Journal of Electromagnetic Waves and Applications*, Vol. 3, No. 4, 359–377, 1989.
3. Eyges, L., P. Gianino, and P. Wintersteiner, "Modes of dielectric waveguides of arbitrary cross-sectional shape," *J. Opt. Soc. Am.*, Vol. 698, 1226–1235, 1979.
4. Bagby, J. S., D. P. Nyquist, and B. C. Drachman, "Integral formulation for analysis of integrated dielectric waveguides," *IEEE Trans. Microw. Theory Tech.*, Vol. 33, 906–915, 1985.

5. Galick, A. T., T. Kerkhoven, and U. Ravaioli, "Iterative solution of the eigenvalue problem for a dielectric waveguide," *IEEE Trans. Microw. Theory Tech.*, Vol. 40, 699–705, 1992.
6. Schulz, N., K. Bierwirth, F. Arndt, and U. Koster, "Finite-difference method without spurious solutions for the hybrid-mode analysis of diffused channel waveguides," *IEEE Trans. Microw. Theory Tech.*, Vol. 38, 722–729, 1990.
7. Bierwirth, K., N. Schulz, and F. Arndt, "Finite-difference analysis of rectangular dielectric waveguide structures," *IEEE Trans. Microw. Theory Tech.*, Vol. 34, 1104–1114, 1986.
8. Schweig, E. and W. B. Bridges, "Computer analysis of dielectric waveguides: A finite-difference method," *IEEE Trans. Microw. Theory Tech.*, Vol. 32, 531–541, 1984.
9. Radhakrishnan, K., "Analysis of dielectric waveguides and microstrip lines using Krylov subspace based techniques," Ph.D. Thesis, U. Illinois, Urbana-Champaign, USA, 1999.
10. Radhakrishnan, K. and W. C. Chew, "Efficient analysis of waveguiding structures," *Fast Efficient Algorithms in Comp. Electrom.*, 461–485, Chapter 10, Artech House, Inc., Boston, 2001. Reprinted by EML, Univ. Illinois, 2006.
11. Cendes, Z. J. and P. Silvester, "Full-wave analysis of multiconductor transmission lines on anisotropic inhomogeneous substrates," *IEEE Trans. Microw. Theory Tech.*, Vol. 18, 1124–1131, 1970.
12. Ahmed, S. and P. Daly, "Finite element method for inhomogeneous waveguides," *IEE Proc.*, Vol. 116, 1661–1664, 1969.
13. Chew, W. C. and M. A. Nasir, "A variational analysis of anisotropic, inhomogeneous dielectric waveguides," *IEEE Trans. Microw. Theory Tech.*, Vol. 37, 661–668, 1989.
14. Ikeuchi, M., H. Swami, and H. Niki, "Analysis of open type dielectric waveguide by the finite element iterative method," *IEEE Trans. Microw. Theory Tech.*, Vol. 29, 234–239, 1981.
15. Rahman, B. M. A. and J. B. Davies, "Finite-element analysis of optical and microwave waveguide problems," *IEEE Trans. Microw. Theory Tech.*, Vol. 32, 20–28, 1984.
16. Koshiba, M., K. Hayata, and M. Suzuki, "Approximate scalar finite-element analysis of anisotropic optical waveguides with off-diagonal elements in a permittivity tensor," *IEEE Trans. Microw. Theory Tech.*, Vol. 32, 587–593, 1984.
17. Lee, J. F., D. K. Sun, and Z. J. Cendes, "Full-wave analysis of dielectric waveguides using tangential vector finite elements," *IEEE Trans. Microw. Theory Tech.*, Vol. 39, 1262–1271, 1991.

18. Lee, J. F., "Finite element analysis of lossy dielectric waveguides," *IEEE Trans. Microw. Theory Tech.*, Vol. 42, 1025–1031, 1994.
19. Feynman, R., R. B. Leighton, and M. L. Sands, *The Feynman Lectures on Physics*, Vol. I, Chapter 52, Addison-Wesley Publishing Co., 1965.
20. Chew, W. C., *Waves and Fields in Inhomogeneous Media*, IEEE Press, 1995.
21. Chew, W. C., "Inhomogeneously filled waveguides," *Theory of Guided Waves*, Note of Course at U. Illinois, Urbana-Champaign, 2012.
22. Warnick, K. F., R. H. Selfridge, and D. V. Arnold, "Teaching electromagnetic field theory using differential forms," *IEEE Trans. Educ.*, Vol. 40, 53–68, Feb. 1997.
23. Flanders, H., *Differential Forms with Applications to the Physical Sciences*, Dover Publications, Mineola, NY, 1963.
24. Tarhasaari, T. and L. Kettunen, "Some realizations of a discrete Hodge operator: A reinterpretation of finite element techniques," *IEEE Trans. Magn.*, Vol. 35, 1494–1497, 1999.
25. Teixeira, F. L. and W. C. Chew, "Lattice electromagnetic theory from a topological viewpoint," *J. Math. Phys.*, Vol. 40, 169–187, 1999.
26. Bossavit, A., "Whitney forms: A class of finite elements for three-dimensional computations in electromagnetism," *IEE Proc.*, Vol. 135, 493–500, 1998.
27. Bossavit, A., "Generating Whitney forms of polynomial degree one and higher," *IEEE Trans. Magn.*, Vol. 38, 314–344, 2000.
28. He, B. and F. L. Teixeira, "On the degree of freedom of lattice electrodynamics," *Phys. Lett. A*, Vol. 336, 1–7, 2005.
29. He, B. and F. L. Teixeira, "Geometric finite element discretization of Maxwell equations in primal and dual spaces," *Phys. Lett. A*, Vol. 349, 1–14, 2006.
30. He, B., "Compatible discretizations for Maxwell equations," Ph.D. Thesis, Ohio State U., USA, 2006.
31. Kim, J. and F. L. Teixeira, "Parallel and explicit finite-element time-domain method for Maxwell's equations," *IEEE Trans. Antennas Propag.*, Vol. 59, 2350–2356, 2011.
32. Rao, S. M., D. R. Wilton, and W. A. Glisson, "Electromagnetic scattering by arbitrarily shaped three dimensional homogeneous lossy dielectric objects," *IEEE Trans. Antennas Propag.*, Vol. 30, 409–418, 1982.

33. Buffa, A. and S. Christiansen, "A dual finite element complex on the barycentric refinement," *Math. Comput.*, Vol. 40, 1743–1769, 2007.
34. Chen, Q. and D. R. Wilton, "Electromagnetic scattering by three-dimensional arbitrary complex material/conducting bodies," *Antennas Propag. Soc. Int. Symp.*, 1990.
35. Andriulli, F. P., K. Cools, H. Bagci, F. Olyslager, A. Buffa, S. Christiansen, and E. Michielssen, "A multiplicative Calderon preconditioner for the electric field integral equation," *IEEE Trans. Antennas Propag.*, Vol. 56, 2398–2412, 2008.
36. Grote, M. J. and T. Huckle, "Parallel preconditioning with sparse approximate inverses," *SIAM J. Sci. Comp.*, Vol. 18, 838–853, 1997.
37. Goell, J. E., "A circular-harmonic computer analysis of rectangular dielectric waveguides," *Bell Syst. Tech. J.*, Vol. 48, 2133–2160, 1969.
38. Yang, J. J., G. E. Howard, and Y. L. Chow, "A simple technique for calculating the propagation dispersion of multiconductor transmission lines in multilayer dielectric media," *IEEE Trans. Microw. Theory Tech.*, Vol. 40, 622–627, 1992.